

Docket No.: 060188-0570



PATENT

IN THE UNITED STATES PATENT AND TRADEMARK OFFICE

In re Application of : Customer Number: 20277
Katsuki NAGAHASHI, et al. : Confirmation Number: 4471
Application No.: 10/632,960 : Group Art Unit: 2138
Filed: August 04, 2003 : Examiner: Siddiqui, Saqib Javaid
:

For: ACCELERATED TEST METHOD FOR FERROELECTRIC MEMORY DEVICE

REQUEST FOR CERTIFICATE OF CORRECTION UNDER 37 CFR 1.323

Mail Stop COC
Commissioner for Patents
P.O. Box 1450
Alexandria, VA 22313-1450

Sir:

*Certificate
JAN 19 2007
of Correction*

In reviewing the above-identified patent, a printing error was discovered therein requiring correction in order to conform the Official Record in the application. The error was made in good faith and was of a clerical or typographical nature or of minor character.

The error noted is set forth on the two attached copies of form PTO-1050 Rev. 2-93 in the manner required by the Commissioner's Notice.

Specifically, On the title page of the Letters Patent, under section "(56) References Cited, U.S. PATENT DOCUMENTS", add – 5,337,279 8/1994 Gregory et al. –, and under section "(56) References cited, OTHER PUBLICATIONS", change "Polarization Fatigue Characteristics of Sol-Gel Ferroelectric" to --Polarization Fatigue Characteristics of Sol-Gel Ferroelectric Pb_{(Zr_{0.4}Ti_{0.6})O₃} Thin-Film Capacitors --. For your immediate reference attached are photocopies of the two 1449's filed and the two references.

01/17/2007 JADDO1 00000093 500417 7111218
01 FC:1811 100.00 DA

Please charge the \$100.00 filing fee to our Deposit Account 500417.

Please charge any shortage in fees due in connection with the filing of this paper to Deposit Account 500417 and please credit any excess fees to such deposit account.

Respectfully submitted,

McDERMOTT WILL & EMERY LLP

Michael E. Fogarty
Registration No. 36,139

**Please recognize our Customer No. 20277
as our correspondence address.**

600 13th Street, N.W.
Washington, DC 20005-3096
Phone: 202.756.8000 MEF:JGH
Facsimile: 202.756.8087
Date: January 16, 2007

UNITED STATES PATENT AND TRADEMARK OFFICE
CERTIFICATE OF CORRECTION

PATENT NO. : 7111210
DATED : September 19, 2006
INVENTOR(S) : Katsuki NAGAHASHI, et al.

It is certified that an error appears in the above-identified patent and that said Letters Patent is hereby corrected as shown below:

On the title page of the Letters Patent,

Under section "(56) References Cited, U.S. PATENT DOCUMENTS", add --
5,337,279 8/1994 Gregory et al. --

Under section "(56) References cited, OTHER PUBLICATIONS", change
"Polarization Fatigue Characteristics of Sol-Gel Ferroelectric" to --
Polarization Fatigue Characteristics of Sol-Gel Ferroelectric Pb (Zr_{0.4}Ti_{0.6})O₃
Thin-Film Capacitors --

MAILING ADDRESS OF SENDER:
McDermott Will & Emery LLP
600 13th Street, NW
Washington, DC 20005
USA

PATENT NO.
7,111,210

No. of add'l copies
@ 50¢ per page

{ _____

JAN 19 2007,

UNITED STATES PATENT AND TRADEMARK OFFICE
CERTIFICATE OF CORRECTION

PATENT NO. : 7111210
DATED : September 19, 2006
INVENTOR(S) : Katsuki NAGAHASHI, et al.

It is certified that an error appears in the above-identified patent and that said Letters Patent is hereby corrected as shown below:

On the title page of the Letters Patent,

Under section "(56) References Cited, U.S. PATENT DOCUMENTS", add --
5,337,279 8/1994 Gregory et al. --

Under section "(56) References cited, OTHER PUBLICATIONS", change
"Polarization Fatigue Characteristics of Sol-Gel Ferroelectric" to --
Polarization Fatigue Characteristics of Sol-Gel Ferroelectric Pb $(\text{Zr}_{0.4}\text{Ti}_{0.6})\text{O}_3$
Thin-Film Capacitors --

MAILING ADDRESS OF SENDER:
McDermott Will & Emery LLP
600 13th Street, NW
Washington, DC 20005
USA

PATENT NO.
7,111,210

No. of add'l copies
@ 50¢ per page
{ _____ }



SHEET 1 OF 1

INFORMATION DISCLOSURE CITATION IN AN APPLICATION

(PTO-1449)

ATTY. DOCKET NO.
60188-570SERIAL NO.
not yet assignedAPPLICANT
Katsuki NAGAHASHI, et al.FILING DATE
August 04, 2003GROUP
not yet assigned

U.S. PATENT DOCUMENTS

EXAMINER'S INITIALS	CITE NO.	Document Number Number-Kind Codes (if known)	Publication Date MM-DD-YYYY	Name of Patentee or Applicant of Cited Document	Pages, Columns, Lines, Where Relevant Passages or Relevant Figures Appear
	US				

FOREIGN PATENT DOCUMENTS

EXAMINER'S INITIALS	CITE NO.	Foreign Patent Document Country Code - Number - Kind Codes (if known)	Publication Date MM-DD-YYYY	Name of Patentee or Applicant of Cited Document	Pages, Columns, Lines Where Relevant Figures Appear	Translation	
						Yes	No
SS	A	11-174026 with English abstract	07/02/1999	Fujitsu Ltd.			

OTHER ART (including Author, Title, Date, Pertinent Pages, Etc.)

EXAMINER'S INITIALS	CITE NO.	Include name of the author (in CAPITAL LETTERS), title of the article (when appropriate), title of the item (book, magazine, journal, serial, symposium, catalog, etc.), date, page(s), volume-issue number(s), publisher, city and/or country where published.
SS	7A	"Polarization Fatigue Characteristics of Sol-Gel Ferroelectric", Takashi Mihara et al., Jpn. J. Appl. Phys. Vol. 33 (1994) pp. 3996-4002, Part 1, No 7A, July 1994

EXAMINER

DATE CONSIDERED
12/2/2005

*EXAMINER: Initial if reference considered, whether or not citation is in conformance with MPEP 609. Draw line through citation if not in conformance and not considered.
Include copy of this form with next communication to applicant.

1 Applicant's unique citation designation number (optional). 2 Applicant is to place a check mark here if English language Translation is attached.



SHEET 1 OF 1

INFORMATION DISCLOSURE
CITATION IN AN
APPLICATION

(PTO-1449)



ATTY. DOCKET NO.
60188-570

SERIAL NO.
10/632,960

APPLICANT
Katsuki NAGAHASHI, et al.

FILING DATE
August 04, 2003

GROUP
2858

U.S. PATENT DOCUMENTS

EXAMINER'S INITIALS	CITE NO.	Document Number Number-Kind Code(s) (if known)	Publication Date MM-DD-YYYY	Name of Patentee or Applicant of Cited Document	Pages, Columns, Lines, Where Relevant Passages or Relevant Figures Appear
	US	5,337,279	08/09/1994	Gregory et al.	
	US				

FOREIGN PATENT DOCUMENTS

EXAMINER'S INITIALS	CITE NO.	Foreign Patent Document Country Codes - Number + - Kind Codes (if known)	Publication Date MM-DD-YYYY	Name of Patentee or Applicant of Cited Document	Pages, Columns, Lines Where Relevant Figures Appear	Translation	
						Yes	No
SS		WO 01/22426 A1	03/29/2001	CELIS SEMICONDUCTOR CORPORATION			
SC		EP 0 836 197 A2	04/15/1998	MATSUSHITA ELECTRONICS CORPORATION			
SC		DE 100 58 779 A1	08/13/2002	INFINEON TECHNOLOGIES AG			x

OTHER ART (Including Author, Title, Date, Pertinent Pages, Etc.)

EXAMINER'S INITIALS	CITE NO.	Include name of the author (in CAPITAL LETTERS), title of the article (when appropriate), title of the item (book, magazine, journal, serial, symposium, catalog, etc.), date, page(s), volume-issue number(s), publisher, city and/or country where published.	
CS		TRAYNOR S.D., et al. "Capacitor test simulation of retention and imprint characteristics for ferroelectric memory operation." Integrated Ferroelectrics, New York, NY, vol. 16, 1997, pages 63-78, XP-002099258	

EXAMINER

DATE CONSIDERED

12/22/05

*EXAMINER: Initial if reference considered, whether or not citation is in conformance with MPEP 609. Draw line through citation if not in conformance and not considered.
Include copy of this form with next communication to applicant.

1 Applicant's unique citation designation number (optional). 2 Applicant is to place a check mark here if English language Translation is attached.

Polarization Fatigue Characteristics of Sol-Gel Ferroelectric Pb_{(Zr_{0.4}Ti_{0.6})O₃} Thin-Film Capacitors

Takashi MIHARA, Hitoshi WATANABE and Carlos A. PAZ DE ARAUJO¹

Applied Research Dept., Corporate Research Division, Olympus Optical Co., Ltd., Hachioji-shi, Tokyo 192

¹University of Colorado at Colorado Springs and Symmetrix Corporation, Colorado Springs, Colorado 80918, USA

(Received November 8, 1993; accepted for publication April 16, 1994)

Fatigue characteristics of PbZr_{0.4}Ti_{0.6}O₃ (PZT) thin-film capacitors made by sol-gel spin coating have been evaluated using hysteresis measurement by bipolar continuous pulses. The following three stages were found according to the cumulative polarization switching cycles: (1) slow fatigue stage at the initial switching cycles, (2) logarithmic fatigue stage at middle switching cycles which is recognized in general, (3) saturated stage at extremely large number of switching cycles. The decays of the nonswitched parts started in the middle of the logarithmic fatigue stage. The switching cycles at half of the initial remanent polarization are exponentially proportional to reverse electric field, and the degradation is explained in terms of an "electric-field-activating process" with an accelerating factor of 1.2×10^{-3} in units of decade kV/cm on our PZT thin-film capacitors. Temperature dependence of fatigue characteristics was unexpectedly small and activation energy was estimated to be 0.051 eV. A plausible fatigue model is proposed in which injected charge initiates the polarization fatigue.

KEYWORDS: Ferroelectrics, thin film, PZT, fatigue, polarization degradation, bipolar pulses, hysteresis loops, electric field, temperature, fatigue model

1. Introduction

Recently, ferroelectric thin films such as lead zirconate titanate (PZT) have gathered much attention for use in non-volatile memories.^{1,2)} However, several problems of reliability such as ferroelectric fatigue,³⁾ depolarization effect^{4,5)} and imprint property^{6,7)} have served as major obstacles to the commercialization of ferroelectric devices, as well as process integration with the CMOS process. Polarization fatigue, in particular, which is characterized as the degradation of remanent polarization by polarization reversal (polarization switching), is the most important problem because it affects the number of write and read cycles which is required to extend the application of ferroelectric memory. The understanding and the improvement of this polarization fatigue might be keys to the commercialization of high density ferroelectric memories. However, these characteristics, to date, are not well understood and thus the physical mechanism could not be established.

Several reports have presented electrical characteristics of fatigue: Melnick *et al.*,^{8,9)} Schuele and Traynor,¹⁰⁾ Lipeles *et al.*,¹¹⁾ Naik *et al.*,¹²⁾ and Watanabe *et al.*¹³⁾ measured the degradation of remanent polarization by fatigue at a certain applied voltage on their PZT thin-film capacitors. According to these papers, fatigue evaluation was only carried out as part of the examination of electric properties, thus no detailed evaluation results or descriptions were given. Mihara *et al.*¹⁴⁾ and Nasby *et al.*⁴⁾ measured the applied voltage dependence of fatigue characteristics and showed that the phenomenon was an electric-field-activating process.

Turning to microscopic characterization and theoretical approach, Scott *et al.*¹⁵⁾ studied the switching time after fatigue on KNO₃ thin-film capacitors. Bullington *et al.*¹⁶⁾ studied optical characterization of fatigued thin-film PZT lateral capacitors. Duiker *et al.*³⁾ studied a theoretical model of fatigue based upon impact ioniza-

tion. The last group found three discrete regions including the initial decay of remanent polarization at an early stage of switching cycles. Araujo *et al.*¹⁷⁾ studied the degradation mechanism using a two-state cluster model which could explain our experimentally measured results.¹⁴⁾ Recently, Sesu and Yoo¹⁸⁾ and Raymond *et al.*¹⁹⁾ reported the fatigue model based on defect chemistry, in which oxygen vacancy played an important role.

In this study, we explain the detailed experimental results of the fatigue on PZT thin-film capacitors using hysteresis measurements after polarization switching cycles.

2. Sample Preparation

The samples used for this study are PZT ceramic thin films which were prepared using the sol-gel spin-coating technique. A platinum bottom electrode with a titanium adhesive layer was deposited on the silicon oxide layer on Si wafer. Then PZT sol-gel was deposit-

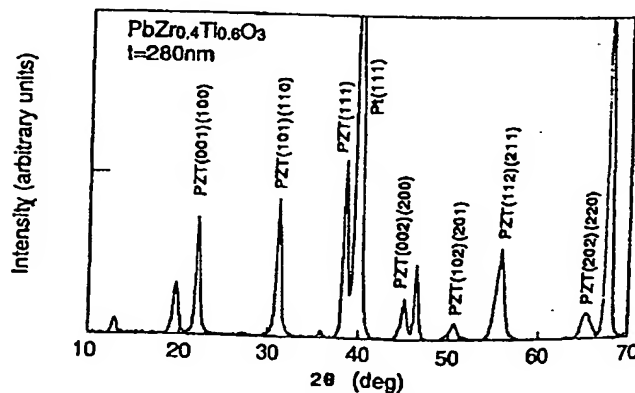


Fig. 1. X-ray diffraction pattern of sol-gel-fabricated PbZr_{0.4}Ti_{0.6}O₃ ferroelectric thin-film capacitors. This pattern has no dominant peaks which indicate specific orientation, and is supposed to have a polycrystalline structure.

ed on the bottom electrode by the spin-coating method. Perovskite ferroelectric phase was obtained by annealing at 650°C for 30 min in an oxygen furnace. A top platinum electrode was then deposited by sputtering and patterned using ion-milling techniques. Figure 1 shows the typical X-ray diffraction pattern of the prepared PZT thin film. Since this texture has no dominant orientation, our sol-gel PZT thin film is polycrystalline. The grain size ranges from 40 nm to 70 nm. The thickness of samples is about 280 nm. The area of the capacitors is $100 \mu\text{m} \times 100 \mu\text{m}$ ($1 \times 10^{-4} \text{ cm}^2$).

3. Evaluation Methods

Fatigue was evaluated by measuring the hysteresis loops after a certain number of polarization reversals induced by bipolar pulse waves. The switching endurance tests were carried out with a circuit shown in Fig. 2(a). DUT is the capacitor measured in this study, C_{load} load capacitor, V_m input pulses, and V_m output monitor signals. The capacitance of this load capacitor was taken to be about 100 times larger than the capacitance of DUT, so that about 99% of voltage of the input pulse was applied to the ferroelectric capacitor. The typical frequency of input pulses was 1 MHz and pulse width was 500 ns, which was about three times longer than the switching time t_s (the time required for transfer of 90% of the charge into the external element) of our ferroelectric capacitors. All input pulses consist of positive and negative pulses with the same pulse

height, so that the polarization of each fatigue step could be reversed completely.

Hysteresis measurements were carried out by the conventional Sawyer-Tower circuit using a 1 kHz sine curve without any compensation. Figures 2(b) and 2(c) show the schematic measurement circuit and hysteresis loop, respectively. The extracted hysteresis parameters are illustrated in Fig. 2(c). $P_{r+}-P_{r-}$ is defined as the difference between the positive remanent polarization (P_{r+}) and negative one (P_{r-}), and $E_{c+}-E_{c-}$ the difference between the positive coercive field (E_{c+}) and negative one (E_{c-}); P_{s+} and P_{s-} are positive and negative saturated polarizations, respectively.

4. Evaluation Results

4.1. Hysteresis parameters after fatigue

Figure 3 shows several hysteresis loops consisting of the initial state before fatigue and fatigued states after certain switching cycles. The initial state had a well-saturated hysteresis loop, in which $P_{r+}-P_{r-}$ is about $32 \mu\text{C}/\text{cm}^2$ and the coercive field is about $45 \text{ kV}/\text{cm}$. After a certain amount of switching cycles with pulse height of ± 6 volts ($212 \text{ kV}/\text{cm}$), the hysteresis loops shrank gradually. Figure 4 through Fig. 7 show several hysteresis parameters as functions of cumulative switching cycles to obtain the quantitative change of ferroelectric properties induced by fatigue. These figures are expressed in terms of logarithm of switching cycles on the X-axis, which is generally used by other researchers.⁸⁻¹²⁾ It is useful to evaluate the characteristic change over a wide range of switching cycles in view of engineering. Thus, we have evaluated them over an extremely wide range from 10 cycles to 10^9 cycles. Figure 4 shows $P_{r+}-P_{r-}$, P_{r+} and $-P_{r-}$ as functions of cumulative switching cycles. The pulse height is ± 8 volts ($282 \text{ kV}/\text{cm}$), which is about two times as large as the electric field in normal ferroelectric memory operation, and the frequency is 1 MHz. $P_{r+}-P_{r-}$ had a normal logarithmic decay, as described in the former reports.⁸⁻¹²⁾ However, since we evaluated over a wide range of switching cycles, we could observe three stages in this figure according to the cumulative switching cycles as follows.

(1) Slow fatigue stage: this stage ranged from 10 cycles to 3×10^5 cycles in this case, which was characterized by the slow decay of $P_{r+}-P_{r-}$. The cycle dependence of $P_{r+}-P_{r-}$ obeys the log scale with a slow rate. The logarithmic coefficient is about $0.55 \mu\text{C}/\text{decade}$ or $1.7\%/\text{decade}$. Note that no initial decay of $P_{r+}-P_{r-}$ at an early stage of switching cycles was found on our PZT thin-film capacitor, which was different from the result in ref. 3.

(2) Logarithmic fatigue stage: this stage corresponded to the cumulative switching cycles ranging from 3×10^5 to 1×10^8 cycles in this case, which was commonly recognized by many researchers. In this stage, $P_{r+}-P_{r-}$ is proportional to the logarithm of the cumulative switching cycles.

(3) Saturated stage: this stage corresponded to the cumulative switching cycles beyond 1×10^8 cycles in this case. After the logarithmic stage, $P_{r+}-P_{r-}$ was satu-

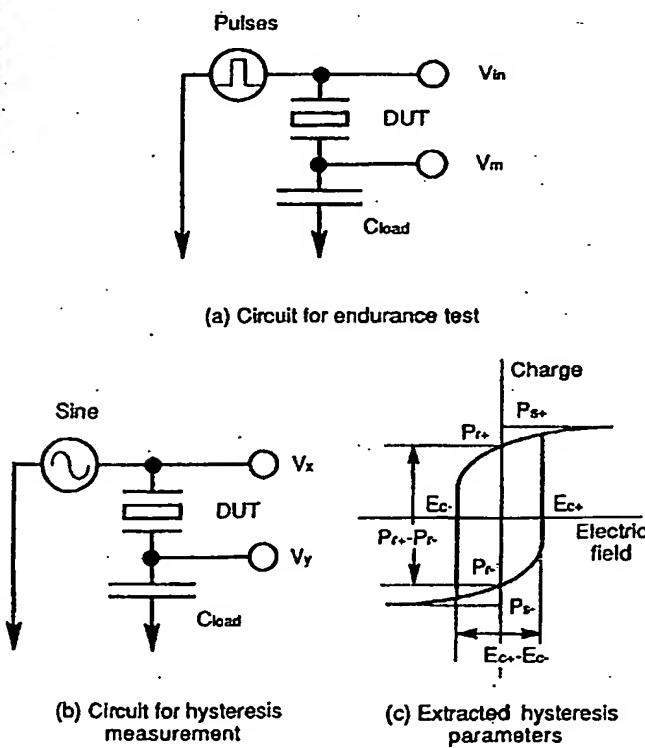


Fig. 2. Schematic circuits and extracted hysteresis parameters used in this study. (a) The circuit for endurance test, (b) the circuit for hysteresis loop measurement, where DUT is ferroelectric capacitor, and (c) definition of the extracted hysteresis parameters.

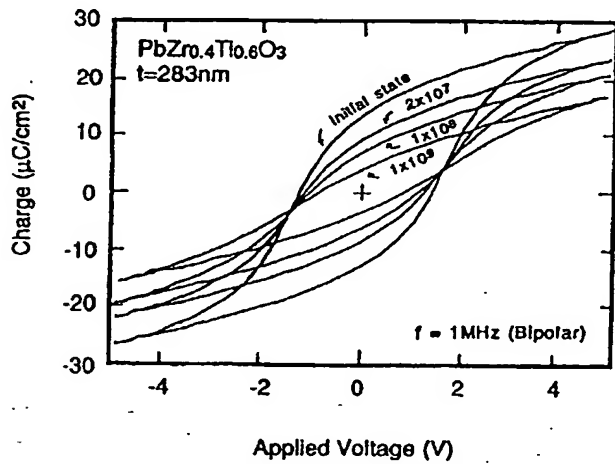


Fig. 3. Hysteresis loops depicting an initial state and fatigued states at certain polarization switching cycles. Applied pulse height during endurance test was 6 V (212 kV/cm). Hysteresis loops shrank with cumulative switching cycles.

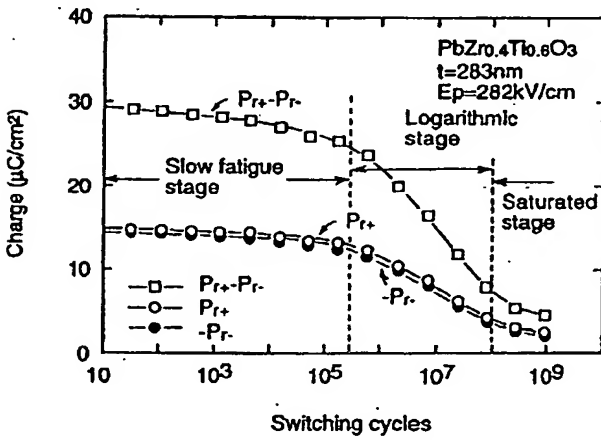


Fig. 4. Remanent polarizations ($P_{r+}, -P_{r-}$, $P_{r-}, -P_{r+}$) as functions of cumulative polarization switching cycles. Polarization fatigue characteristics are distinguished into three stages.

rated to about $5 \mu\text{C}/\text{cm}^2$, which was about 16% of the initial value.

Figure 4 also shows the positive remanent polarization (P_{r+}) and negative one ($-P_{r-}$) as functions of cumulative switching cycles. Note that P_{r+} and $-P_{r-}$ behave similarly. This means that the hysteresis loop exhibits good symmetry along the charge axis of hysteresis loops through all stages. Figure 5 shows the saturated polarization ($P_{s+}, -P_{s-}$) in conjunction with remanent polarization ($P_{r+}, -P_{r-}$) as functions of switching cycles. All parameters show similar dependence in the slow fatigue stage and the logarithmic stage. Note, however, that the saturated polarizations ($P_{s+}, -P_{s-}$) continue decreasing at the saturated stage, while remanent polarizations ($P_{r+}, -P_{r-}$) tend toward saturation. Figure 6 shows the nonswitched parts of hysteresis loops, which are obtained by subtracting P_r from P_s . A nonswitched part consists of two

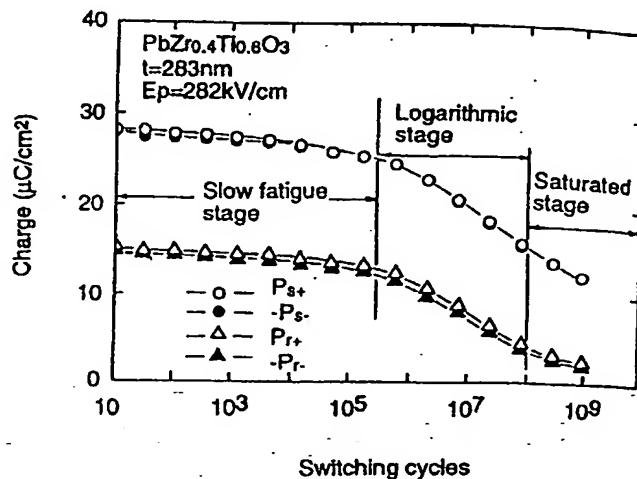


Fig. 5. Saturated polarizations ($P_{s+}, -P_{s-}$) and remanent polarizations ($P_{r+}, -P_{r-}$) as functions of cumulative polarization switching cycles. The saturated polarizations decreased through logarithmic fatigue stage and saturated stage.

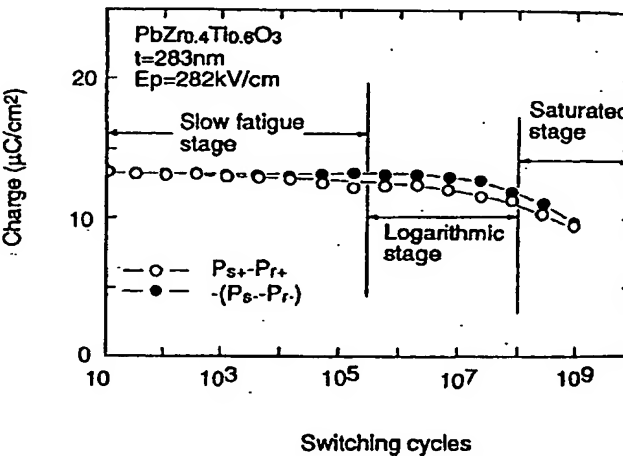
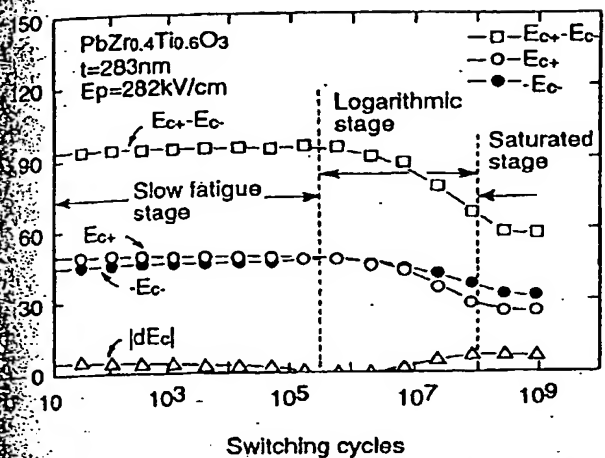


Fig. 6. Nonswitched parts of hysteresis loops as functions of cumulative polarization switching cycles. The nonswitched parts started to decrease in the middle of the logarithmic stage.

parts: back-switching from biased-saturated state to zero-bias state, and discharge by the linear capacitance. The nonswitched parts of polarization are almost constant from the slow fatigue stage up to the middle of the logarithmic stage, but show a monotonous decrease from the middle of the logarithmic stage to the saturated stage.

Figure 7 shows the coercive fields, such as $E_{c+} - E_{c-}$, E_{c+} , $-E_{c-}$ and $|dE_c|$, as functions of cumulative switching cycles. The parameter dE_c is defined as the difference between E_{c+} and $-E_{c-}$, which will be governed by several factors, such as anisotropic internal stress, internal field induced by inhomogeneity of remanent polarization, and internal field arising from asymmetrical distribution of space charges. $E_{c+} + E_{c-}$, E_{c+} and $-E_{c-}$ show no significant change at the slow fatigue stage. This means the shape of hysteresis loop does not



Coercive fields ($E_{c+} + E_{c-}$, E_{c+} , $-E_{c-}$, dE_c) as functions of cumulative polarization switching cycles. $E_{c+} + E_{c-}$, E_{c+} and $-E_{c-}$ varied with the three stages. The symmetry of hysteresis loops in terms of space charge field (dE_c) was increased at the logarithmic fatigue stage, and saturated at the saturated stage.

change at this stage. Note that these parameters decrease at the logarithmic fatigue stage, indicating that the shape of the hysteresis loop is significantly changed. Note that $-E_{c-}$ becomes larger than E_{c+} , and $|dE_c|$ is increased at the logarithmic fatigue stage, which means the hysteresis curve has shifted toward the negative side (or bottom-electrode side).

Pulse height dependence of degradation

Pulse height dependence of fatigue characteristics is extremely important in view of engineering and survey of their physical properties. Figure 8 shows remanent polarization as a function of cumulative switching cycles with respect to the applied pulse height ranging from 177 kV/cm to 318 kV/cm. Here pulse height means the absolute value of an amplitude for incident pulses during the endurance test. Hence all $P_{r+} - P_{r-}$ values were measured with the same amplitude of 212 kV/cm. Fatigue characteristics drastically varied with the pulse height. Note that the pulse height changed only at the start of the logarithmic stage, and no changes were found over the slow fatigue stage. Note that the tangents of $P_{r+} - P_{r-}$ at the logarithmic fatigue stage showed no significant changes with pulse height. Three stages were also found in the fatigue curves, as described above. This characteristic strongly implies that the degradations of $P_{r+} - P_{r-}$ by fatigue possess an "electric-field-activating process". Figures 9 and 10 show other presentations of this property, that is, an applied pulse height dependence of $N(50\%)$, which is defined as the specific cycle at which $P_{r+} - P_{r-}$ decays to 50% of the initial $P_{r+} - P_{r-}$ value. Figure 9 shows $N(50\%)$ as a function of pulse height, while Fig. 10 shows the same as a function of the reciprocal of pulse height. The two samples (A and B) in these figures are the capacitors from different wafers, but the fabrication processes and annealing conditions were exactly the same. Generally speaking, these figures are useful

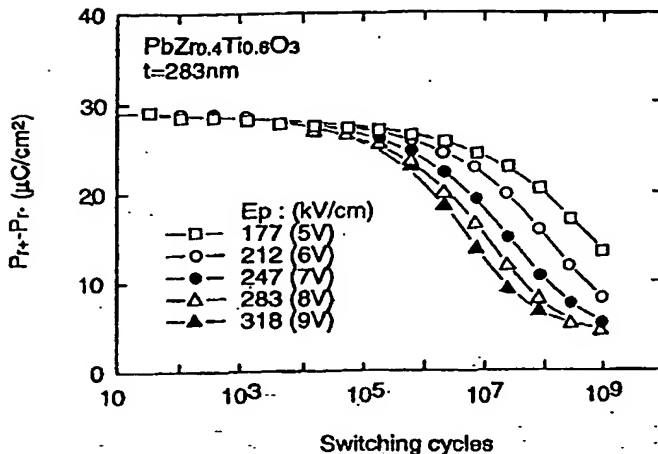


Fig. 8. Remanent polarization $P_{r+} - P_{r-}$ as a function of cumulative switching cycles with respect to applied pulse height. Applied pulse height changed at the early steps of the logarithmic fatigue stage.

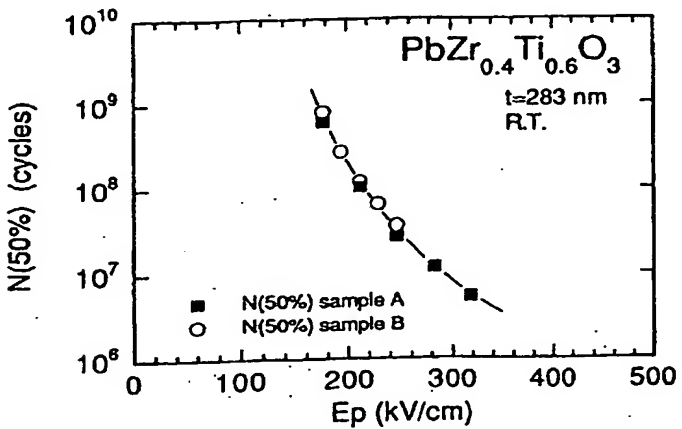


Fig. 9. $N(50\%)$ as a function of applied pulse height in electric field during endurance test. $N(50\%)$ is defined as the specific cycle at which $P_{r+} - P_{r-}$ decays to 50% of the initial $P_{r+} - P_{r-}$ value.

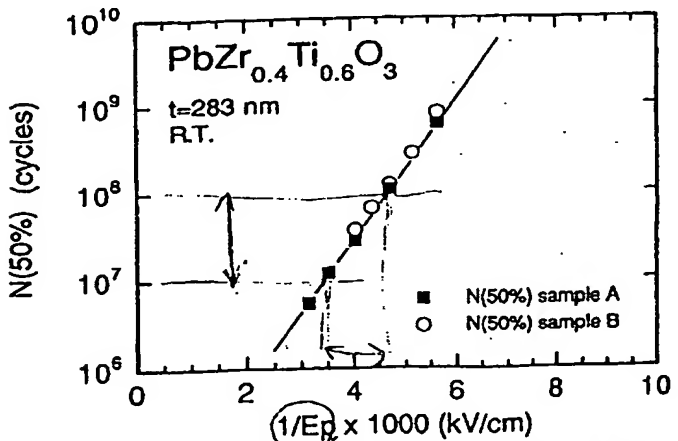


Fig. 10. $N(50\%)$ as a function of reciprocal of pulse height. All data points were fitted to the straight line. The acceleration factors were estimated as 1.23×10^{-3} and 1.20×10^{-3} (decade/kV/cm) for samples A and B, respectively.

to estimate the lifetime of the capacitor when it is forced into a specific applied pulse in some applications. Therefore, it is important to clarify which dependence the degradation of $P_{r+}-P_{r-}$ obeys. Consequently, the dependence on the reciprocal of pulse height, as shown in Fig. 10, gave a better fit to the straight line obtained by the least-squares method, indicating that the logarithm of $N(50\%)$ was reciprocally proportional to pulse height. The fitting result is

$$N(50\%) = 1.47 \times 10^4 \exp\left(\frac{1876}{E_p}\right) \quad (1)$$

for sample A, and

$$N(50\%) = 1.47 \times 10^4 \exp\left(\frac{1918}{E_p}\right) \quad (2)$$

for sample B, where E_p is the pulse height (kV/cm). To estimate the impact of the pulse height, an acceleration factor should be specified in the reciprocal of the pulse height. The acceleration factor is defined by the change of the required independent variable in order to vary the dependent variable to ten times its initial value in this paper. This is shown as follows:

$$\text{Factor} = \frac{\partial\left(\frac{1}{E_p}\right)}{\partial \log[N(50\%)]} = 2.302 \frac{\partial\left(\frac{1}{E_p}\right)}{\partial \ln[N(50\%)]}. \quad (3)$$

Utilizing eqs. (1), (2) and (3), the acceleration factors were calculated to be 1.23×10^{-3} and 1.20×10^{-3} in units of decade kV/cm for samples A and B, respectively, which means that $N(50\%)$ increases ten times with every additional increase of 1.23×10^{-3} to the value of $1/E_p$ for sample A. Equations (1) and (2) also enable us to estimate lifetime for a specific application. If we use this capacitor under 3.0 V (106 kV/cm) operation, the $N(50\%)$ is estimated to be about 7×10^{11} cycles for sample A.

4.3 Temperature dependence of $P_{r+}-P_{r-}$ degradation

Temperature dependence of ferroelectric properties must be one of the most important characteristics in view of not only engineering but also physical properties. Generally speaking, temperature dependence can be used to determine the activation process of this degradation mechanism. Figure 11 shows $P_{r+}-P_{r-}$ as a function of cumulative switching cycles at different temperatures. The significant change by temperature is manifested by the difference of the values of $P_{r+}-P_{r-}$ at the slow fatigue stage, in which the initial $P_{r+}-P_{r-}$ value decreased with increase of the temperature. $P_{r+}-P_{r-}$ decreased to 70% of the initial (unfatigued) value as the temperature was increased from room temperature to 150°C. All fatigue curves had almost the same tendency except their absolute value of $P_{r+}-P_{r-}$. Note that the temperature dependence of logarithmic stage was not significant. This result was very different from that in ref. 3, in which low temperature led to fast degradation. Since our samples were made by the sol-gel method, the repeatability of this tendency on the different samples was quite good.

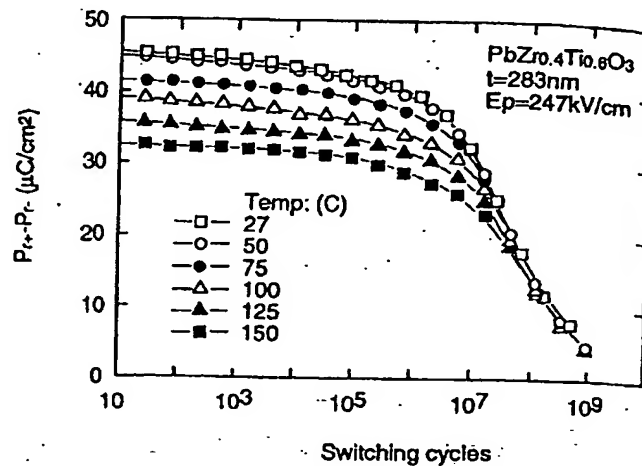


Fig. 11. Remanent polarization $P_{r+}-P_{r-}$ as a function of cumulative polarization switching cycles at different temperatures. There was no significant change except the values of $P_{r+}-P_{r-}$ at the slow fatigue stage.

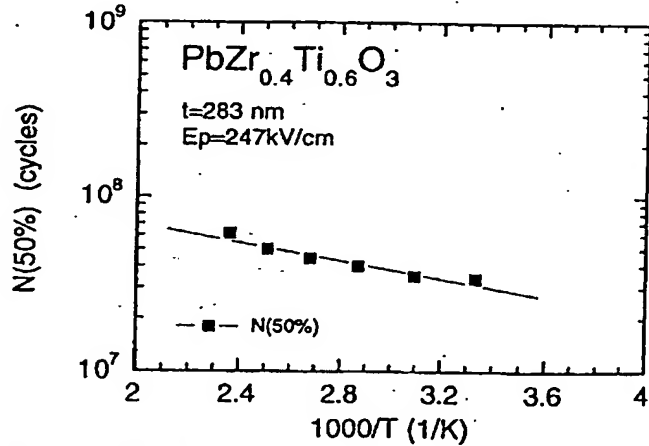


Fig. 12. $N(50\%)$ as a function of reciprocal of temperature. The activation energy of this degradation was estimated to be 0.051 eV, which was an unexpectedly small value.

Figure 12 shows $N(50\%)$, which is described in §4.2, as a function of the reciprocal of temperature. $N(50\%)$ slightly decreased with temperature. However, this dependence is not as significant as that of pulse height. Utilizing this reciprocal dependence of temperature, the activation energy of this degradation was estimated to be 0.051 eV, which was an unexpectedly small value.

5. Discussion

In this section, we discuss several subjects found in this study, and a new fatigue model is described.

5.1 Three stages in polarization fatigue

The three stages found in this study are completely different from those in ref. 3. Our PZT capacitors showed no initial degradation at the early stage of switching cycles. We believe that ferroelectric capaci-

tors fabricated by appropriate processes show well-saturated hysteresis loops and do not exhibit such initial degradation. The fact that we obtained three stages on the fatigue curve may not be so easy to understand. All parameters and hysteresis loops did not change until the start of the logarithmic stage, and showed a sudden decrease with the logarithm of switching cycles in this figure. $P_{r+}-P_{r-}$ saturates at a relatively large value, which is about 16% of the initial one at the saturated stage. The logarithmic fatigue stage has been reported,^{3,8-14)} but no report has been made on the existence of three stages, especially the saturated stage. The nonswitched part of the hysteresis loop shows a decrease at the middle of the logarithmic stage. This means that the influence of dielectric constant lowering (including back-switching) came later than the degradation of remanent polarization, and dielectric constant was not as sensitive as P_r . At the saturated stage, the nonswitched parts kept decreasing with the same ratio, while $P_{r+}-P_{r-}$ tended toward saturation.

Turning to the symmetry of the hysteresis loop during the endurance test, as shown in Fig. 7, although its shift along the polarization axis was not significant, that along the electric field was found to be significant in this study. This shift is thought to correspond to the generated internal electric field caused by asymmetrical distribution of space charges or inhomogeneity of remanent polarization arising from a large number of polarization switching cycles. This asymmetry is frequently found in the PZT samples before the second high-temperature annealing, which is performed after deposition of the top electrode. The asymmetry is also recognized in samples after imprint evaluation, wherein the capacitor is exposed to a large number of unipolar pulses without polarization switching.⁷⁾ This asymmetry was increased at the logarithmic fatigue stage and saturated, similarly to the case of $P_{r+}-P_{r-}$. This generated internal field may be caused by the imbalance of space charges at the interface layer near the electrode arising from fatigue, as explained by Okazaki and co-worker in bulk ferroelectric BaTiO₃,^{20,21)} using switching current measurements after fatigue and aging. Assuming that the imbalance of space charge is a major reason, the internal field generated by space charges is about 7 kV/cm. Then the asymmetry of built-in potential (dV_b) is estimated to be 0.2 V assuming that space charges exist at the interface and $dV_b = dE_i/t$, where t is the thickness of ferroelectric film.

5.2 Electric field dependence of degradation

An electric-field-activating process implies that the fatigue mechanism is caused by charged particles such as carriers, ions and charged defects. In addition to this, the electric field changed only at the start of the logarithmic fatigue stage, and degradation rate did not change in this stage. It is well known that lead in PZT is easily volatilized. When PbO is evolved from PZT upon high-temperature annealing, both donors arising

from oxygen vacancies and acceptors arising from Pb vacancies will be produced, as mentioned by Smyth and co-workers.^{19,22)} Then, the surfaces adjacent to electrodes tend to become semiconducting or insulating, possessing some amount of space charge, as recognized by Kanzig.²³⁾ Therefore, we believe that the space charge plays an important role to explain this electric-field-activating process.

5.3 Temperature dependence of degradation

An extremely small activation energy of 0.051 eV was estimated, which was only about one-tenth that of electrical conductivity, ranging from 0.33 eV²⁴⁾ to about 0.4 eV in our samples. Furthermore, an activation energy of temperature dependence on lifetime under DC electric field was reported as 1.37 eV.¹⁸⁾ We note that fatigue does not obey the thermal activation mechanism as reported by Sesu and Yoo.¹⁸⁾ This indicates that the fatigue mechanism is not directly influenced by the amount of carriers or the thermal activating process over the trapping level of defects.

5.4 Plausible fatigue model called "charge injection model"

Taking the electric field dependence into account, and from an analogy of physical models for silicon oxide breakdown,²⁵⁾ we consider that the polarization fatigue is initiated by a specific carrier injection. Injection takes place in ferroelectric thin film at early steps of the logarithmic fatigue stage. The injection process is specified by "Fowler-Nordheim tunneling", and the amount of injected charge per second is given by

$$Q = AE_i^2 \exp\left(\frac{B}{E_i}\right), \quad (4)$$

where A and B depend on the electron effective mass and barrier height at the injecting interface, and E_i is an electric field at the interface. This charge injection takes place the moment polarization switching occurs, in which the local internal electric field becomes much larger than the external field. We assumed that the localized high electric field was generated at the interface or at the defective area due to polarization reversal in conjunction with space charges in the surface layer and the defective area. Under this localized high electric field, the injected charge gains high energy so that the energetically charged particles collide with ions and generate new defects and space charges. Only "Fowler-Nordheim tunneling" of the fatigue-initiating process can explain the reciprocal relation of applied electric field and the lack of temperature dependence. We called this model the "charge injection model". In this paper, we used several assumptions on the localized electric field. We will discuss these in conjunction with conductivity mechanism in another paper.

The three stages in polarization fatigue can be explained by the charge injection model as follows. An initiation of charge injection does not occur by the end of the slow fatigue stage. The initiation of charge injection takes place at early steps of the logarithmic

fatigue stage. The start of charge injection varies with pulse height and other conditions. Once the charge injection starts, a positive feedback due to energy gain and defect generation (space charges) may occur, as described above, and degradation takes place easily. As the switching cycles increase, the remanent polarization is gradually degraded. Then the local electric field at the surface or the defective area becomes weaker, and charge injection slows down. This slowdown is recognized as the saturated stage.

6. Conclusions

We have studied the fatigue characteristics of sol-gel ferroelectric $\text{Pb}(\text{Zr}_{0.4}\text{Ti}_{0.6})\text{O}_3$ thin-film capacitors by measuring hysteresis loops after polarization switching. We found three stages in the polarization degradation curve as follows: (1) slow fatigue stage at initial switching cycles, (2) logarithmic fatigue stage at middle switching cycles which was recognized in general, (3) saturated stage at extremely large switching cycles. We also separated switched parts and non-switched parts from hysteresis loops as functions of switching cycles, the decays of nonswitched parts started in the middle of the logarithmic stage. An asymmetry of the hysteresis loop with electric field was also found, which coincided with the logarithmic fatigue stage. The degradation of remanent polarization strongly depended upon an applied electric field, and was explained in terms of an "electric-field-activating process". $N(50\%)$, which is defined as the specific cycle at which $P_{r+}-P_{r-}$ decays to 50% of the initial value, was reciprocally proportional to the pulse height, and the acceleration factor was about 1.2×10^{-3} decade kV/cm. Fatigue degradation had no significant temperature dependence. A plausible fatigue model called the "charge injection model" was proposed.

- 1) J. F. Scott and C. A. Araujo: *Science* **246** (1989) 1400.
- 2) J. F. Scott, C. A. Araujo and L. D. McMillan: *Proc. 1989 Ultrasonic Symp.* (1989) p. 299.
- 3) H. M. Dulker, P. D. Beal, J. F. Scott, C. A. Araujo, B. M. Melnick, J. D. Cuchiro and L. D. McMillan: *J. Appl. Phys.* **11**

(1990) 151.

- 4) R. D. Nasby, J. R. Schwank, M. S. Rodgers and S. L. Miller: *Proc. 3rd Int. Symp. Integrated Ferroelectrics*, Colorado Springs (1991) p. 376.
- 5) N. Abt: *Proc. 3rd Int. Symp. Integrated Ferroelectrics*, Colorado Springs (1991) p. 404.
- 6) J. M. Benedetto, R. A. Moore and F. B. McLean: *Proc. 3rd Int. Symp. Integrated Ferroelectrics*, Colorado Springs (1991) p. 44.
- 7) T. Miura, H. Watanabe and C. A. Araujo: *Jpn. J. Appl. Phys.* **32** (1993) 4168.
- 8) B. M. Melnick, C. A. P. Araujo, L. D. McMillan, D. A. Carver and J. F. Scott: *Ferroelectrics* **116** (1991) 79.
- 9) B. M. Melnick, M. C. Scott, C. A. Araujo, L. D. McMillan and T. Miura: *Proc. 4th Int. Symp. Integrated Ferroelectrics*, Monterey (1992) p. 221.
- 10) P. J. Schuele and S. D. Traynor: *Abstr. Fifth U.S.-Japan Semin. Dielectric and Piezoelectric Ceramics* (1990) p. 286.
- 11) R. A. Lipeles, B. A. Morgan and M. S. Leung: *Proc. 3rd Int. Symp. Integrated Ferroelectrics*, Colorado Springs (1991) p. 368.
- 12) I. K. Naik, L. E. Sanchez, S. Y. Wu and B. P. Madreric: *Proc. 3rd Int. Symp. Integrated Ferroelectrics*, Colorado Springs (1991) p. 431.
- 13) H. Watanabe, T. Miura, H. Yoshimori and C. A. Araujo: *Proc. 3rd Int. Symp. Integrated Ferroelectrics*, Colorado Springs (1991) p. 346.
- 14) T. Miura, H. Watanabe, H. Yoshimori, C. A. Araujo, B. M. Melnick and L. D. McMillan: *Proc. 3rd Int. Symp. Integrated Ferroelectrics*, Colorado Springs (1991) p. 116.
- 15) J. F. Scott, B. Poulingue, K. Dimmler, M. Parris, D. Buler and S. Eaton: *J. Appl. Phys.* **62** (1987) 4510.
- 16) J. F. Bullington, M. D. Ivey and J. T. Evans: *Proc. CMC89* (1989) p. 201.
- 17) C. A. Araujo, R. Zuleeg, T. Miura, H. Watanabe, A. Carrico, L. D. McMillan and J. F. Scott: *Proc. 3rd Int. Symp. Integrated Ferroelectrics*, Colorado Springs (1991) p. 151.
- 18) S. B. Sesu and I. K. Yoo: *Proc. 4th Int. Symp. Integrated Ferroelectrics*, Monterey (1992) p. 640.
- 19) M. V. Raymond, J. Chen and D. M. Smyth: to be published in *Proc. 5th Int. Symp. Integrated Ferroelectrics*, Colorado Springs (1993).
- 20) K. Okasaki and K. Sakata: *ETJ Jpn.* **7-1** (1962) 13.
- 21) K. Okasaki: *Soc. Electron.* **78-850** (1959) 905 [In Japanese].
- 22) D. M. Smyth: *Ferroelectrics* **116** (1991) 117.
- 23) W. Kanzig: *Phys. Rev.* **98** (1955) 549.
- 24) R. Moazzami, C. Hu and W. H. Shepherd: *IEEE Trans. Electron Devices* **39** (1992) 2044.
- 25) S. Holland, I. C. Chen, T. P. Ma and C. Hu: *IEEE Electron Device Lett.* **EDL-5** (1984) 302.

**This Page is Inserted by IFW Indexing and Scanning
Operations and is not part of the Official Record**

BEST AVAILABLE IMAGES

Defective images within this document are accurate representations of the original documents submitted by the applicant.

Defects in the images include but are not limited to the items checked:

- BLACK BORDERS**
- IMAGE CUT OFF AT TOP, BOTTOM OR SIDES**
- FADED TEXT OR DRAWING**
- BLURRED OR ILLEGIBLE TEXT OR DRAWING**
- SKEWED/SLANTED IMAGES**
- COLOR OR BLACK AND WHITE PHOTOGRAPHS**
- GRAY SCALE DOCUMENTS**
- LINES OR MARKS ON ORIGINAL DOCUMENT**
- REFERENCE(S) OR EXHIBIT(S) SUBMITTED ARE POOR QUALITY**
- OTHER:** _____

IMAGES ARE BEST AVAILABLE COPY.

As rescanning these documents will not correct the image problems checked, please do not report these problems to the IFW Image Problem Mailbox.